*Mon. Not. R. astr. Soc.* (1983) **205**, 417–434

# Analysis of nebulosity in the planetary nebula NGC 40

R. E. S. Clegg and M. J. Seaton *Department of Physics and Astronomy, University College London, Gower Street, London WC1 6BT*

M. Peimbert★ and S. Torres-Peimbert★ *Instituto de Astronomia, Universidad Nacional Autónoma de México*

Received 1983 February 26; in original form 1982 October 14

**Summary.** Optical and *IUE* spectra of a bright region of nebulosity in the planetary nebula NGC 40 have been combined for an analysis of the physical conditions and abundances in the nebula. Resulting abundances – log $A$ (C) = 9.0, log $A$ (O) = 8.9 and log $A$ (N) = 8.4 – are typical of planetary nebulae and indicate that the nebulosity does not share the extreme abundances of the Wolf–Rayet WC8 central star.

The continuum observed in the *IUE* spectra at an offset position can be fitted well to a calculated nebular continuum; the nebular lines are measured relative to the continuum and hence put on the same scale as optical lines measured relative to Hβ. The absence of stellar features in the offset spectra show that the optical depth for scattering by dust is less than 0.06. The emission in C IV λ1549 from the nebula is anomalously strong. It may be explained, in part, as due to resonance scattering of radiation from the star or from the inner part of the nebula.

New recombination lines of C II are identified in *IUE* spectra; their intensities relative to C II λλ 4267, 7230 in NGC 40 and IC 418 are analysed.

## 1 Introduction

NGC 40 (Perek-Kohoutek 120 + 9°1) is a low-excitation planetary nebula which has been analysed previously by Aller & Czyzak (1979), Kaler (1978) and Aller *et al.* (1972). Its structure is irregular and inhomogeneous, and Aller & Czyzak noted that 'the excitation level changes dramatically from point to point'. The nebular radius, deduced from photographs taken in Hβ or [O III] light, is about 24 arcsec, but recently Louise (1981) detected a faint halo of nebulosity in Hα + [N II] light extending to about 60 arcsec from the central star and filamentary emission about 70–100 arcsec north-east of the nebula. Louise suggested

★ Visiting Astronomers, Kitt Peak National Observatory (operated by the Association of Universities for Research in Astronomy, Inc., under contract with the National Science Foundation).

that the filament might be the result of the interaction between the wind from the central star and the interstellar medium.

The central star of NGC 40 is a bright, 10th magnitude Wolf–Rayet of type WC8. Benvenuti, Perinotto & Willis (1981) observed its ultraviolet spectrum with *IUE*; their preliminary analysis of the P-Cygni profiles seen gave a wind terminal velocity $v_\infty = 2370\,\mathrm{km\,s^{-1}}$ and the remarkable abundance ratio C/He ~ 0.2, with probably no hydrogen. No results for the carbon abundance in the nebula itself have been derived previously. For this low-excitation object, the abundant C ions are expected to be $C^+$ and $C^{++}$, both of which have collisionally-excited lines falling in the range of the *IUE* satellite spectrograph. It is of interest to determine whether the nebula has been affected by the C-rich high-velocity wind from the WC8 star and whether the central star's envelope was ejected after or before becoming extremely C-rich.

In this paper we report on results obtained from combined optical and *IUE* spectra of a patch of nebulosity within NGC 40, located about 14 arcsec north-west of the star. This patch is the brightest on an electronographic map of the nebula (Fig. 1), taken in Hβ light, which was kindly given to us by Dr N. K. Reay. We discuss the observations, the determination of reddening and physical conditions, and the deduction of nebular abundances. Two unexpected features of the *IUE* spectra – strong C IV emission and newly-identified recombination lines of C II – are also discussed.


**Figure 1.** Contour map in Hβ of NGC 40, supplied by Dr N. K. Reay. The position used for the *IUE* aperture is shown by an oval and the positions a and b used for optical observations are shown by rectangles. North is to the top and east to the left. The complete figure is of size 63 arcsec north–south, 49 arcsec east–west. The contour spacing is linear.

## 2 Observations

### 2.1 OPTICAL

The observations were carried out in 1980–81 with the 2.1-m telescope at Kitt Peak National Observatory and the Intensified Image Dissector Scanner (IIDS). The observational procedure has been described before (Torres-Peimbert & Peimbert 1977). The dual entrance

**Table 1.** Observed fluxes $F(\lambda)$ for optical spectra of regions a and b.

| $\lambda$ | Identification | NGC 40$_a$ $\log \frac{F(\lambda)}{F(H\beta)}$ | NGC 40$_b$ $\log \frac{F(\lambda)}{F(H\beta)}$ |
|---|---|---|---|
| $f(3646^-)$ | H I + ... | − 2.45 | − 2.48 |
| $f(3646^+)$ | H I + ... | − 3.30 | − 3.32 |
| $f$(Bac) | H I | − 2.52 | − 2.55 |
| 3726 + 3729 | [O II] | + 0.42 | + 0.42 |
| 3835 | H 9 | − 1.32 | − 1.31 |
| 3868 + 3869 | He I + [Ne III] | − 2.60 | − 2.62 |
| 3889 | H 8 + He I | − 1.01 | − 1.01 |
| 3967 + 3970 | [Ne III] + H 7 | − 0.96 | − 0.96 |
| 4026 | He I | − 2.10 | − 2.16 |
| 4068 + 4076 | [S II] | − 1.62 | − 1.63 |
| 4102 | H$\delta$ | − 0.72 | − 0.72 |
| 4267 | C II | − 2.46 | − 2.45 |
| 4340 | H$\gamma$ | − 0.41 | − 0.41 |
| 4363 | [O III] | − 2.91:: | − 2.95:: |
| 4388 | He I | − 2.60: | − 2.72: |
| 4471 | He I | − 1.69 | − 1.74 |
| 4562 + 4571 | [Mg II] + Mg I | − 2.09 | − 2.07 |
| 4658 | [Fe III] + ... | − 2.09 | − 2.04 |
| 4861 | H$\beta$ | 0.00 | 0.00 |
| 4921 | He I | − 2.21 | − 2.23 |
| 4959 | [O III] | − 1.23 | − 1.21 |
| 5007 | [O III] | − 0.73 | − 0.71 |
| 5198 + 5200 | [N I] | − 2.14 | − 2.19 |
| 5270 | [Fe III] | − 2.75: | − 2.61: |
| 5518 | [Cl III] | − 2.51: | − 2.70: |
| 5538 | [Cl III] | − 2.40: | − 2.50: |
| 5755 | [N II] | − 1.57 | − 1.56 |
| 5876 | He I | − 1.05 | − 1.07 |
| 6300 | [O I] | − 1.36 | − 1.41 |
| 6311 | [S III] | − 2.10: | − 2.16: |
| 6363 | [O I] | − 1.82 | − 1.89 |
| 6548 | [N II] | + 0.14 | + 0.13 |
| 6563 | H$\alpha$ | + 0.70 | + 0.70 |
| 6583 | [N II] | + 0.65 | + 0.66 |
| 6678 | He I | − 1.52 | − 1.51 |
| 6717 | [S II] | − 0.82 | − 0.81 |
| 6731 | [S II] | − 0.64 | − 0.63 |
| 7065 | He I | − 1.64 | − 1.61 |
| 7136 | [Ar III] | − 1.18 | − 1.15 |
| 7231 + 7236 | C II | − 1.91: | − 2.17: |
| 7281 | He I | − 2.08: | − 2.21: |
| 7320 | [O II] | − 0.93 | − 0.95 |
| 7330 | [O II] | − 1.03: | − 1.00: |
| | $\log F(H\beta)_{obs}$ | − 11.62 | − 11.69 |

slits used correspond to 3.8 x 12.4 arcsec on the plane of the sky, the slits were oriented east–west and the separation between the centres of both slits was 99 arcsec. Several gratings were used that covered the following wavelength ranges: λλ 3400–5200, 4800–6600 and 5600–7400 Å. Each spectrum of about 20 mm is recorded into 1024 channels. The FWHM resolution was 3.8 channels (~ 7 Å).

Three regions were observed: a, b and the central star. Regions a and b are located 15 arcsec west, 7 arcsec north and 15 arcsec west, 11 arcsec north relative to the central star respectively (see Fig. 1). NGC 40 and the standard stars were observed alternately in each slit. Measurements of the sky were obtained at the same time with the other slit. Each beam was treated independently and in all cases the sky was subtracted from the source. The data were reduced to absolute fluxes using the standard stars observed by Stone (1977) and Oke (1974). The continuum contribution to each emission line was subtracted by interpolating the continuum on both sides of the emission line.

Table 1 gives absolute Hβ fluxes in erg $cm^{-2} s^{-1}$ and fluxes of other lines relative to Hβ. Also in this table we present the observed continuum intensities near the Balmer discontinuity, $f(\lambda)$ in erg $s^{-1} cm^{-2} Å^{-1}$; where $f(3646^-) - f(3646^+) = f(\mathrm{Bac})$, since the contribution shortwards and longwards of the Balmer discontinuity due to two photon emission and other H and He continua cancel out in the subtraction. By comparing the intensity ratios of two different observing seasons we estimated that the standard deviation, $\sigma$, was smaller than 0.04 dex for all the intensities relative to Hβ with the exception of those marked with a colon where $\sigma < 0.08$ dex and those with two colons where $\sigma < 0.12$ dex.

The C II λ 4267 Å line is present both in the central star and in regions a and b. Since the line is very weak in the nebular regions and is relatively strong in the stellar spectrum we analyse the possibility that a fraction of it is produced by dust scattered light. The relatively high intensities of λ 4686 of He II in the central star and its absence in regions a and b sets an upper limit of 4 per cent for a dust-scattered component of λ 4267 in the nebular region.

In Figs 2–5 we present representative spectra of NGC 40 corresponding to one observing season.

## 2.2 ULTRAVIOLET SPECTRA

The *IUE* satellite was used to obtain low-resolution spectra in the SWP and LWR camera ranges in 1981 November. The large aperture (LAP) was centred 13 arcsec west, 6 arcsec north of the central star; the position angle of the major axis was 32° east of north. The overlap of the LAP with the slits used for optical spectroscopy can be seen in Fig. 1. The useful images obtained were SWP 15412 (70 min) and LWR 11924 (120 min) on November 5 and SWP 15445 (180 min) on November 7. The LAP was positioned by a blind-offset procedure from a nearby guide star, and its centring was checked during each exposure by measurement of other guide stars with the *IUE* fine-error sensor. To an accuracy of about 1–2 arcsec, the LAP had the same position on both days, and the two SWP spectra were averaged. In addition, no significant differences were seen between the SWP spectra except for a defect on SWP 15445 in the wavelength range 1320–1420 Å, caused by a particle event. Only SWP 15412 was used in this range.

We also had access to the *IUE* spectra of the central star, which were kindly lent to us by Dr A. J. Willis. The images – SWP 3074, 3075 and LWR 2656 – are described by Benvenuti *et al.* (1981). These authors also obtained a short exposure with the LAP centred 7.5 arcsec north of the star. All spectra were reduced by us on the VAX computer of the UCL STARLINK node; the extraction procedure followed that described by Harrington *et al.* (1982).

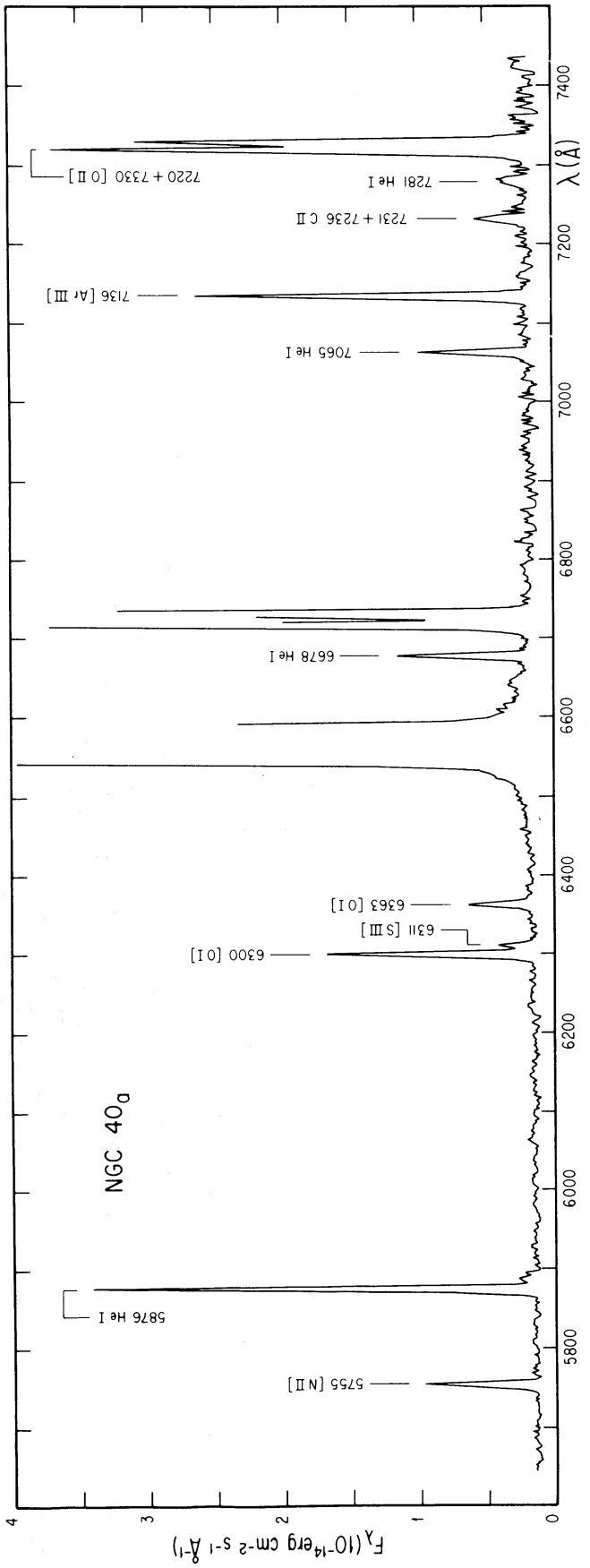


**Figure 2.** Spectrum taken in the red at position a, with vertical scale expanded to show fainter lines.

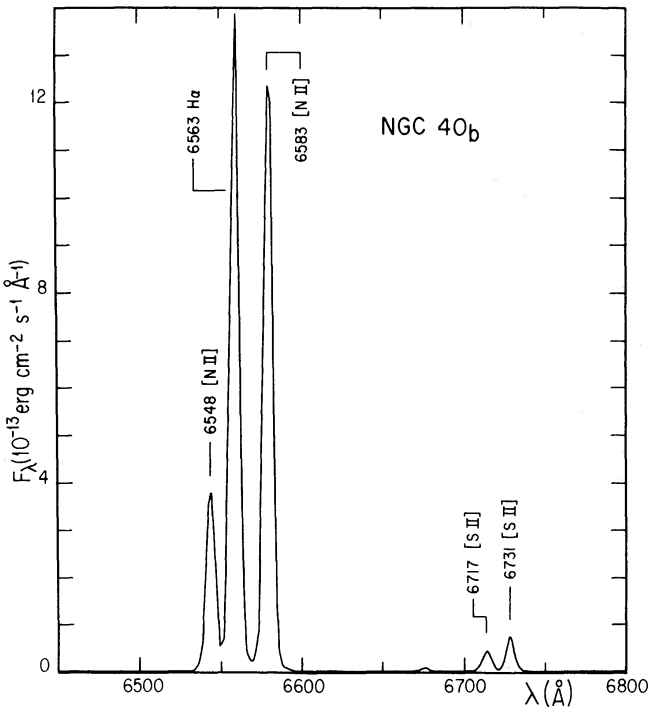


**Figure 3.** Portion of the spectrum taken in the red at position b.

The observed fluxes from averaged spectra, with merging of those from SWP and LWR, are shown on Fig. 6. There are prominent emission lines of C IV, C III, C II and O II and a continuum which is of nebular origin. The flux in the continuum can be calculated relative to that in Hβ. For the calculation we use $n_e = 1400$ cm$^{-3}$ and $T_e = 8300$ K (see Section 3) and $He^+/H^+ = 0.044$ (see Section 4). At this low value of $n_e$, H I $2s \rightarrow 2p$ collisional transfer is of little importance and the continuum flux is insensitive to $n_e$. The continuum flux relative to Hβ is proportional to $T_e^{-1/2}$. By measuring the UV-line fluxes relative to the continuum we are able to put them on the scale, relative to Hβ, used for the optical observations. Since each line can be compared with the continuum at the wavelength of the line, the deduced flux relative to Hβ is independent of the reddening. The wavelength-dependence of the continuum flux depends on the reddening and can be used to estimate the reddening constant $c$(Hβ). Fig. 6 shows the calculated continuum reddened (using the extinction function of Seaton 1979) with two values of $c$: $c = 0.5$ which gives the best continuum fit; and $c = 0.7$ which gives the best fit to Balmer decrements (see Section 3). Fig. 7 shows the calculated continuum and the observed spectra dereddened with $c = 0.5$.

Table 2 gives, from the *IUE* spectra, measured fluxes in the lines and in the continuum

**Table 2.** Emission line and continuum fluxes in *IUE* spectra.

| λ (Å) | Identification | $F$ (obs) ($10^{-13}$ erg cm$^{-2}$ s$^{-1}$) | $F_\lambda$ (cont) ($10^{-13}$ erg cm$^{-2}$ s$^{-1}$ Å$^{-1}$ |
|---|---|---|---|
| 1549 | C IV $^2S-^2P^0$ | 5.3 ± 0.8 | 0.17 ± 0.04 |
| 1749 | N III] $^2P^0-^4P$ | 1.8 ± 0.6 | 0.14 ± 0.03 |
| 1761 | C II $2s\,2p^2\,^2D-2s^2\,3p\,^2P^0$ | 1.4 ± 0.7 | 0.14 ± 0.03 |
| 1908 | C III] $^3P^0-^1S$ | 9.0 ± 0.8 | 0.09 ± 0.02 |
| 2326 | C II] $^4P-^2P^0$ | 8.0 ± 0.7 | 0.05 ± 0.01 |
| 2470 | [O II] $^2P^0-^4S^0$ | 1.9 ± 0.4 | 0.07 ± 0.01 |
| 2836 | C II $2p^2\,^2S-3p\,^2P^0$ | 0.9 ± 0.4 | 0.13 ± 0.02 |

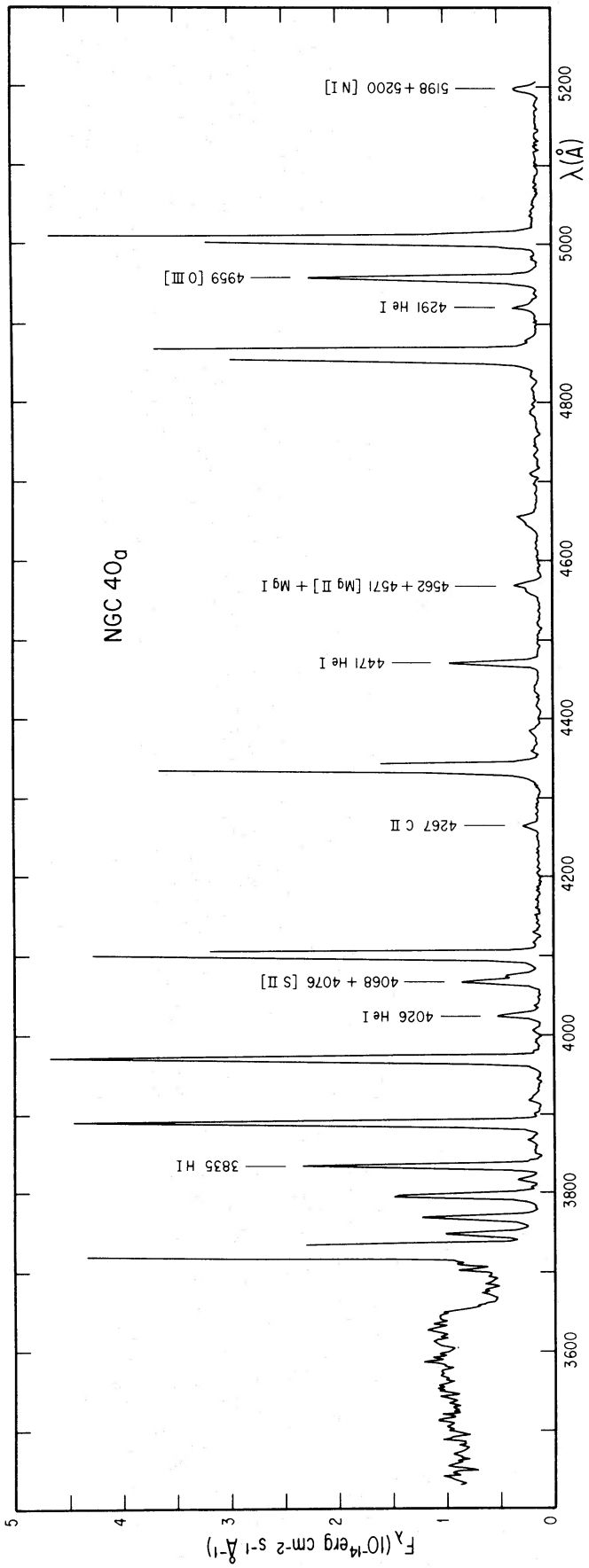


**Figure 4.** Spectrum taken in the blue at position a, with vertical scale expanded to show faint lines and Balmer discontinuity.

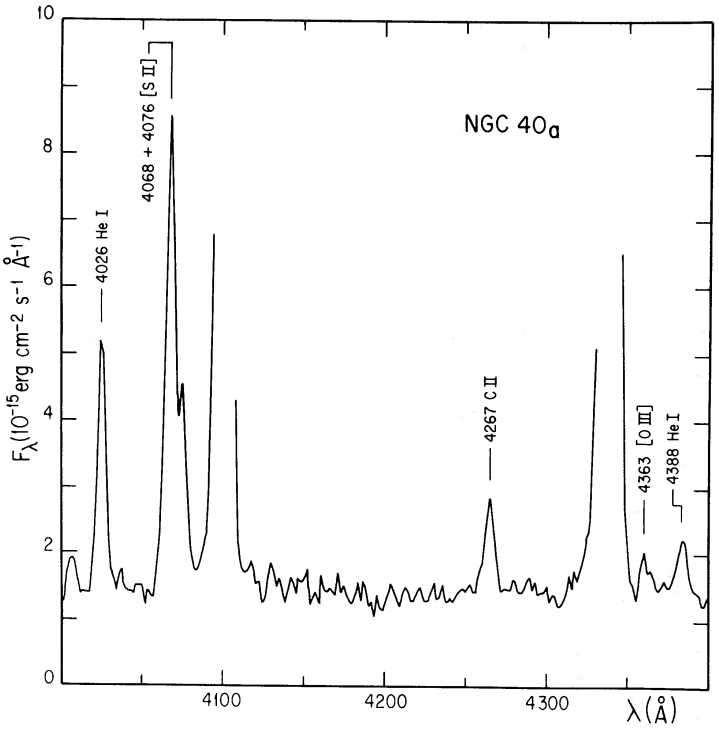


**Figure 5.** Portion of the spectrum taken in the blue at position a showing C II λ 4267 and [O III] λ 4363.

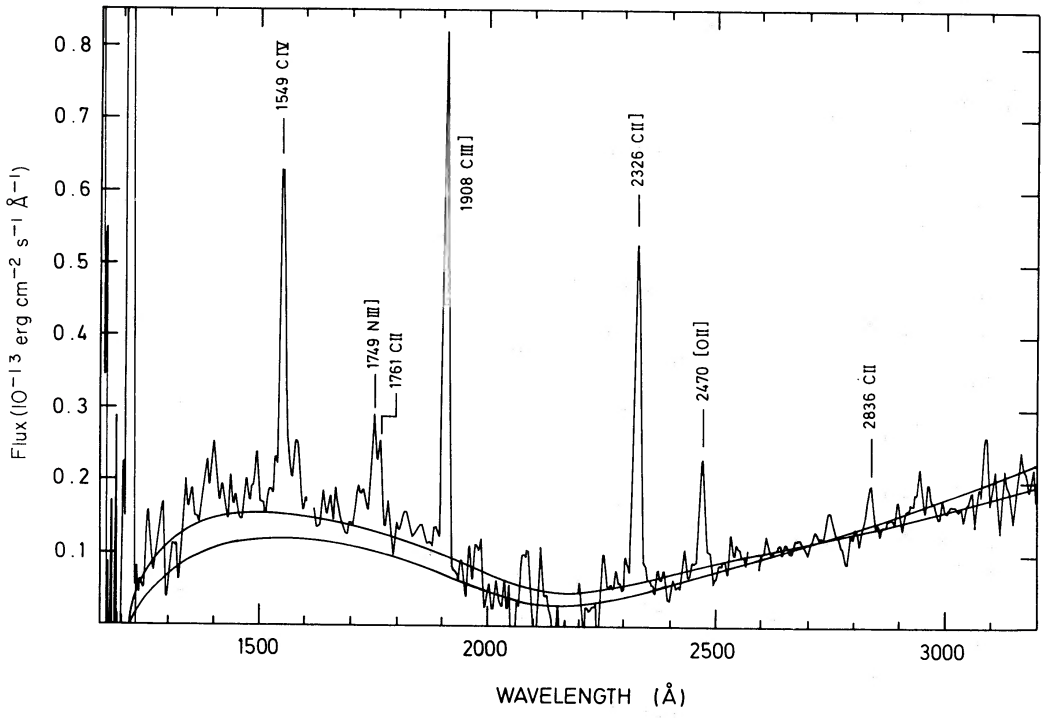


**Figure 6.** Merged *IUE* SWP and LWR spectra. The calculated nebular continuum is shown reddened with $c = 0.5$ (which gives the best fit to the observed continuum) and with $c = 0.7$ (which gives the best fit to the observed Balmer decrement): these two curves are normalized to agree at 2800 Å, and the curve with $c = 0.5$ is the one which has the larger flux at shorter wavelengths.

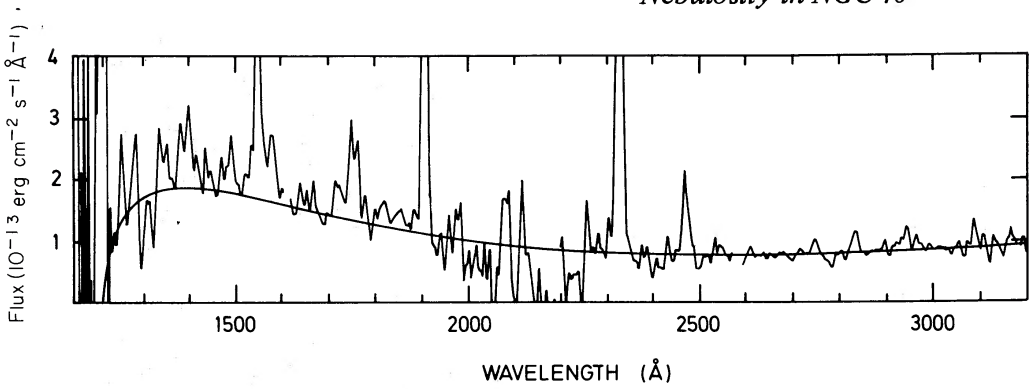


**Figure 7.** The flux from *IUE* corrected for extinction using $c = 0.5$, and the calculated continuum.

and Table 3 includes the deduced fluxes in UV lines, relative to Hβ and corrected for reddening.

Comparison of the stellar and nebular spectra enables us to set an upper limit on the amount of light from the central star scattered by dust within the patch of nebulosity observed. Lines strong in the stellar spectrum, e.g. He II 1640 Å, C III 2297 Å and C IV 2528 Å, are absent from the nebular spectrum. These lines set upper limits of 0.012, 0.006 and 0.007 (respectively) on the fraction of stellar flux seen in the *IUE* LAP. Since the observed nebulosity covers an estimated solid angle fraction $\Omega/4\pi \simeq 0.1$ as seen from the star, then the dust scattering optical depth within the nebulosity is $\tau_D$ (scatt) < 0.06 at 2297 Å.

## 3 Reddening and physics conditions

### 3.1 REDDENING TOWARDS NGC 40

Previous values of the extinction constant $c(H\beta)$ for NGC 40 range from 0.28 (Kaler 1978) to 0.65 (Aller & Czyzak 1979). Since the optical spectra cover a fair wavelength range, λλ 3600–7400 Å, a more precise estimate of $c$ is required. We discuss in turn values obtained from H lines, comparison of radio and Hβ fluxes, the 2200 Å absorption feature and the overall shape of the nebular continuum from 1200 to 3000 Å.

The H line fluxes (Table 1) were compared with the relative fluxes given by Brocklehurst (1971) for the case $n_e = 1400$ cm$^{-3}$, $T_e = 8300$ K. The ratio between Hα and H9 fluxes gives the longest wavelength 'baseline' and yields $c = 0.74 \pm 0.08$ for an assumed error of ±10 per cent in the measured flux ratio. The average value of $c$ for ratios involving $F(H\alpha)$ is $0.72 \pm 0.10$ and that for ratios excluding Hα, $c = 0.76 \pm 0.22$.

The total Hβ and 5 GHz fluxes for the nebula appear rather uncertain. The mean 5 GHz flux, from the data listed by Higgs (1971) is $S = 0.47 \pm 0.07$ Jy. The flux in Hβ is given as $\log F(\beta) = -10.64$ (Liller 1955), although Pottasch *et al.* (1978) quote $\log F(\beta) = -10.45$. We cannot locate the source of this datum. Comparison of radio and Hβ fluxes, for the case $T_e = 8300$ K and $n(He^+)/n(H^+) = 0.07$, gives $c = 0.68$ or 0.88 for $\log F(\beta) = -10.45$ and $-10.64$, respectively.

The strength of the 2200 Å absorption feature has been used to estimate $c$. Pottasch *et al.* (1977) found $c = 0.55$ from the *ANS* satellite data, while Benvenuti *et al.* (1981) obtained $c = 0.6$ using the extinction curve given by Seaton (1979). Our own *IUE* spectra yield $c \geqslant 0.6 \pm 0.1$, but the flux level near 2200 Å is very low and the extraction may have been affected by a noisy background in this region, which is seen on the *IUE* photowrites. Finally, we obtained the best fit to the nebular continuum flux for the case $c = 0.5$, using the Seaton

(1979) mean extinction curve. Adoption of the value $c = 0.7$, suggested by the Balmer decrement, yields fluxes in the SWP range (1200–2000 Å) larger than observed, relative to those in the range 2500–3100 Å. It is possible that the reddening law towards NGC 40 is different from the Galactic average for $\lambda < 2000$ Å. Such a variation at short wavelengths is not uncommon (e.g. Savage & Mathis 1979). However, the DN levels for the continuum are low, and the flux levels are to be regarded as uncertain to within ± 30 per cent for the short-wavelength part of the SWP camera data.

The ratio of $O^+$ line fluxes, $F(2470)/F(7320 + 7330) \equiv R$, was also used to estimate $c$. Using the $A$-values given by Zeippen (1982), we found $R = 1.33$ is the predicted value. Then, $c = 0.42 \pm 0.25$ for a 30 per cent error in the measured ratio. This method is not sensitive because the effective baseline only extends from 4861 to 7330 Å.

For line fluxes in the optical range, we adopt $c = 0.70$. Ultraviolet fluxes relative to the Hβ flux are independent of the reddening law, as explained earlier. Corrected line fluxes, on the scale $F(\mathrm{H}\beta) = 1.0$, are listed by ion in Table 3. Observed fluxes for the regions NGC 40a and 40b were averaged; they are not significantly different and, in addition, the *IUE* LAP covers an area which includes both of them.

### 3.2 $T_e$ AND $n_e$ DETERMINATIONS

The diagnostic line ratios used in determining the electron temperature and density are summarized in Table 4, and the results are displayed in Fig. 8. From the $f$(Bac)/H9 ratio we

**Table 3.** Average corrected fluxes, relative to Hβ. Dereddened with $c = 0.7$.

| Identification | λ (Å) | $\log\{F(\lambda)_{corr}/F(\mathrm{H}\beta)\}$ | Identification | λ (Å) | $\log\{F(\lambda)_{corr}/F(\mathrm{H}\beta)\}$ |
|---|---|---|---|---|---|
| Hα | 6563 | + 0.47 | | | |
| Hβ | 4861 | 0.00 | | | |
| Hγ | 4340 | − 0.32 | N III | 1749 | − 1.06 |
| Hδ | 4101 | − 0.58 | | | |
| H9 | 3835 | − 1.11 | O I | 6300 | − 1.58 |
| | | | | 6363 | − 2.06 |
| He I | 4026 | − 1.96 | | | |
| | 4388 | − 2.57: | O II | 2470 | − 0.97 |
| | 4471 | − 1.64 | | 3726 + 29 | + 0.64 |
| | 4921 | − 2.23 | | 7320 | − 1.24 |
| | 5876 | − 1.21 | | 7330 | − 1.31: |
| | 6678 | − 1.76 | | | |
| | 7065 | − 1.90 | O III | 4363 | − 2.84: |
| | 7281 | − 2.44: | | 4959 | − 1.23 |
| | | | | 5007 | − 0.74 |
| C II | 1761 | − 1.17 | | | |
| | 2326 | − 0.22 | S II | 4068 + 76 | − 1.47 |
| | 2836 | − 1.54 | | 6717 | − 1.07 |
| | 4267 | − 2.34 | | 6731 | − 0.90 |
| | 7231 + 36 | − 2.34: | | | |
| | | | S III | 6311 | − 2.34: |
| C III | 1908 | − 0.26 | | | |
| | | | Fe III | 5270 | − 2.74: |
| C IV | 1549 | − 0.59 | | | |
| | | | Cl III | 5518 | − 2.70: |
| N I | 5198 + 5200 | − 2.21 | | 5538 | − 2.55: |
| N II | 5755 | − 1.70 | Ar III | 7136 | − 1.46 |
| | 6548 | − 0.09 | | | |
| | 6584 | + 0.41 | | | |

**Table 4.** Electron temperature and density results.

| Ion | Ratio | Sensitivity | Result | References |
|---|---|---|---|---|
| O II | $\frac{3726}{3729}$ | $n_e$ | 1400 cm$^{-3}$ | 1 |
| O II | $\frac{7320+30}{3726+29}$ | ($n_e$, $T_e$) | ($T_e$ = 8000 K) | 1 |
| O III | $\frac{4363}{5007+4959}$ | $T_e$ | 10700 ± 1800 K | 2, 3 |
| N II | $\frac{5755}{6548+84}$ | $T_e$ | 7800 K | 4, 5 |
| C III | $\frac{1908}{(C\,II)\,4267}$ | $T_e$ | 8680 K | |
| S II | $\frac{6731}{6717}$ | $n_e$ | 2200 cm$^{-2}$ | 6 |
| S II | $\frac{6717+31}{4068+77}$ | ($n_e$, $T_e$) | ($n_e \sim 3600$ cm$^{-3}$) | 6 |
| Cl III | $\frac{5538}{5518}$ | $n_e$ | 4000 cm$^{-3}$: | 7 |
| H II | Balmer discontinuity | $T_e$ | 8300 (± 1000) K | 8 |

*Note*
The collision strengths used were those adopted by Harrington *et al.* (1980) except as noted in the references below.

*References*
(1) Transition probabilities from Zeippen (1982); (2) Nussbaumer & Storey (1981b); (3) Baluja, Burke & Kingston (1981); (4) Nussbaumer & Rusca (1979); (5) Seaton (1975); (6) Mendoza & Zeippen (1982); (7) Saraph & Seaton (1970) (following their recommendation we reduced the density by 1.5); (8) See Barker (1979).

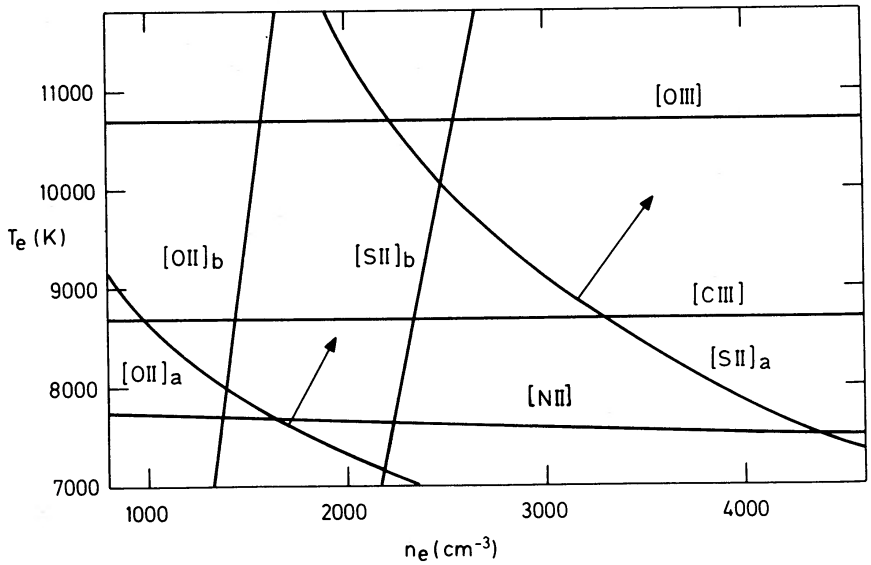


**Figure 8.** Diagram for temperature and density diagnostics, from data of Table 4. The ratios used are: CIII (λ1908)/CII(λ4267); [N II], (λ5755)/λλ6548, 84); [O II] a, (λλ7320, 30)/(λλ3726, 9); [O II] b, (λ3726)/(λ3729); [O III], (λ4363)/(λλ4959, 5007); [S II] a, (λλ6717, 31)/(λλ4068, 77); [S II] b, (λ6731)/(λ6717). The arrows show the effect on [O II] a and [S II] a of varying the reddening from $c = 0.7$ to $c = 0.5$.

derived $T_e$(Balmer) presented in Table 4, where the error corresponds to an error of 0.04 dex in the intensity ratio. The increase of $T_e$ values from $N^+$ to $O^{++}$ is in agreement with the trend found for many other nebulae (Torres-Peimbert & Pembert 1977). The temperature $T_e(C^{++})$ is obtained from the ratio of the collisionally-excited line C III] λ 1908 to the recombination line C II λ 4267. This gives an accurate determination because the ratio $F(1908)/F(4267)$ is very sensitive to $T_e$. It is gratifying that $T_e(C^{++})$ is intermediate between $T_e(N^+)$ and $T_e(O^{++})$.

Electron densities are obtained from the relative strengths of the components of the $^2D$–$^4S$ multiplets in [O II], [S II] and (with larger uncertainty) [Cl III]. The [O II] ratio $R = F(3726)/F(3729)$ was not measured by us but has been taken from Osterbrock (1960), who gave $R = 0.70$ for the 'outer ring *W* of the star', probably our observed patch. In contrast, Aller *et al.* (1972) gives $R = 0.76$ as an average over several regions. We adopted $R = 0.70$.

The only line ratios sensitive to the reddening parameter $c$ are the O II and S II ($^2D$–$^2P$)/($^4S$–$^2D$) ratios. In Fig. 8 we have indicated the change in the solution from these ratios for a change in adopted value of $c(H\beta)$ from 0.7 to 0.5.

Values of $T_e$ for some ions are not measured and therefore have to be assumed. Our estimates are based on ionization potentials. For $N^{++}$ we adopted $T_e = 10\,000$ K, intermediate between values of $C^{++}$ and $O^{++}$. We adopted $T_e(S^{+n}) = T_e(C^{+n})$ because of the similar ionization potentials. For the He recombination lines we took $T_e = T_e$ (Balmer continuum) = 8300 K.

## 4 Abundances

Derived ionic abundances are given in Table 5, together with the adopted value of $T_e$ for each ion and the total C, N, O abundances.

The abundance of ionized He, $He^+/H^+ = 0.044$, gives a lower limit on the total He abundance (it is expected that this low-excitation nebula will contain a substantial amount of neutral helium in the ionized hydrogen region). The relative strengths of the He I recombination lines are in good agreement with the calculations of Brocklehurst (1972) for case B; except that $F(7065)$ is a factor of 2 higher than predicted, which is likely to be due to a large optical depth in the λ 3889 Å line which leads to de-excitation of the 3 $^3P$ level via 3 $^3S$, with emission at 4.1 μm and 7065 Å (Osterbrock 1974).

The total CNO abundances – in logarithmic form $\log A(C) = 9.0$, $\log A(N) = 8.4$ and $\log A(O) = 8.9$ – are not markedly different from those obtained for other planetary nebulae. The nebulosity certainly does not share the extreme abundances of the central star

**Table 5.** Abundances in NGC 40.

| Ion | $T_e$ | $n_i/n(H^+)$ | $n$(Elt)/$n$(H) |
|---|---|---|---|
| $C^+$ | 7 800 | $5.4\times10^{-4}$ | |
| $C^{++}$ | 8 680 | $4.6\times10^{-4}$ | C/H = $1.0\times10^{-3}$ |
| $O^0$ | 7 200 | $2\times10^{-5}$ | |
| $O^+$ | 7 800 | $8.3\times10^{-4}$ | |
| $O^{++}$ | 10 700 | $5.3\times10^{-6}$ | O/H = $8.4\times10^{-4}$ |
| $N^+$ | 7 800 | $1.0\times10^{-4}$ | |
| $N^{++}$ | 10 000 | $1.4\times10^{-4}$ | N/H = $2.4\times10^{-4}$ |
| $S^+$ | 7 800 | $1.6\times10^{-6}$ | |
| $S^{++}$ | 8 680 | $2.3\times10^{-6}$ | S/H = $3.9\times10^{-6}$ |
| $He^+$ | 8 300 | 0.044 | He/H > 0.044 |
| $Cl^{++}$ | 8 680 | $5.1\times10^{-8}$ | |

wind, which has abundance fractions by number He ≃ 83 per cent, C ≃ 17 per cent. The stellar envelope which produced the bulk of the observed nebula does contain processed material, however, since the C and N abundances are higher than solar.

The ratio of carbon to oxygen C/O = 1.1 ± 0.3 is insensitive to *systematic* errors in the adopted $T_e$ values for abundances derived mainly from $C^+$ λ 2326, $C^{++}$ λ1908 and $O^+$ λ 2470. For example, if the values of $T_e$ for $C^+$, $O^+$ and $C^{++}$ in Table 5 are each increased by 1000 K, the C/O ratio only changes from 1.1 to 1.2. The Boltzmann factors for the lines are similar.

Aller *et al.* (1972) have drawn attention to the strength of lines from neutral species such as [N I] and [O I]. Analysis of the [O I] 6300 Å line gives an abundance ratio $O^\circ/H^+ \sim 2 \times 10^{-5}$ for $T_e = 7200$ K (i.e. $O^\circ/O_{total} \sim 2$ per cent). The collision strength was taken from Berrington & Burke (1981). However, the neutral O may be confined to dense condensations within the nebula, in which case an abundance analysis cannot be made.

The S abundance has been obtained with the assumptions $T_e(S^+) = 7800$ K $n_e(S^+) = 3000\ cm^{-3}$ and $T_e(S^{++}) = 8680$ K. As Fig. 8 shows, a consistent solution for $S^+/H^+$ from both the 4070 and 6730 Å lines cannot be obtained. The $S^{+3}$ abundance is estimated to be negligible. The resulting total abundance, $S/H = 4 \times 10^{-6}$, is probably uncertain to within a factor 2.5 because of uncertainties in $T_e$ and $n_e$ and the weakness of the 6312 Å S III line; however, the S abundance is significantly below the solar value $(S/H)_\odot = 1.7 \times 10^{-5}$ (Lambert & Luck 1978). Natta, Panagia & Preite-Martinez (1980) found that the average S/H ratio in 41 planetary nebulae was $6 \times 10^{-6}$. The S deficiency is likely due to condensation in grains. It would be useful to examine whether the S deficiencies are correlated with the nebular C/O ratios, because sulphur chemistry may be rather different in O-rich and C-rich environments. The absence of the Mg II 2800 Å lines in our spectra is surely also due to most of the Mg being in grains.

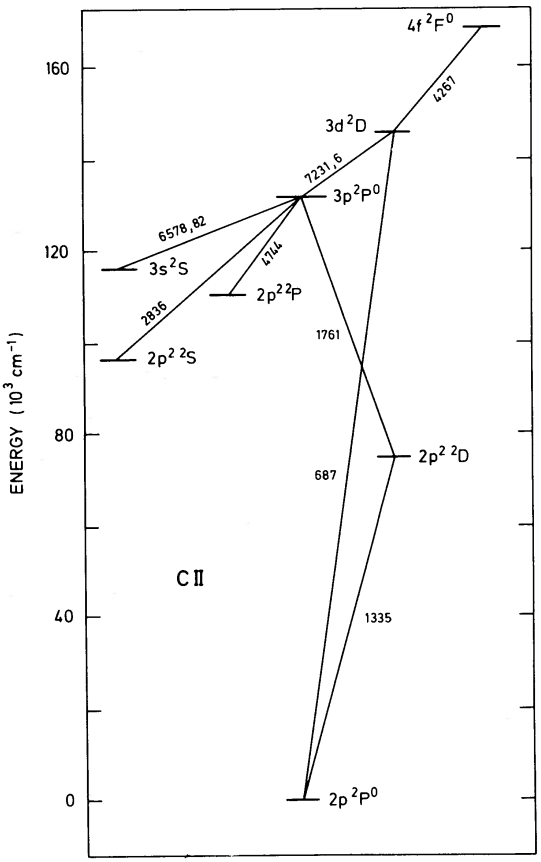


**Figure 9.** Energy levels of C II.

## 5 C II recombination lines

A number of features in our spectra can be identified with C II lines. Fig. 9 shows the relevant transitions on an energy-level diagram.

In the optical spectra of NGC 40 we identify C II $2s^2 3d\ ^2D \rightarrow 2s^2 3p\ ^2P^0$ λλ 7231, 7236 in addition to C II $2s^2 4f\ ^2F^0 \rightarrow 2s^2 3d\ ^2D$ λ 4267. In the *IUE* spectra we identify a feature at λ 1761 with C II $2s^2 3p\ ^2P^0 \rightarrow 2s\,2p^2\ ^2D$ and one at λ 2836 with C II $2s^2 3p\ ^2P^0 \rightarrow 2s\,2p^2\ ^2S$ (the spectra of high-excitation nebulae have an O III Bowen line at λ 2837 but we reject this identification for NGC 40 since its spectra show no other Bowen lines).

We assume that the optically allowed C II lines in NGC 40 are produced by recombination of $C^{++}$. If our identifications are correct, we would expect the lines to be present in the spectra of other nebulae with high $C^{++}$ abundances. We have therefore examined *IUE* low-dispersion spectra of IC 418, both the spectra of Harrington *et al.* (1980) obtained with the aperture centred on the central star and those obtained, using much longer exposures, by Adams & Seaton (1983), with the aperture offset so as to exclude the star. The features at λλ 1761 and 2836 are found to be weakly present in these spectra. In addition C II $2s\,2p^2\ ^2D \rightarrow 2s^2 2p\ ^2P^0$ λ 1335 is seen in the spectra of IC 418, both in the high-dispersion spectra of Clavel, Flower & Seaton (1981) and the low-dispersion offset spectra, but these lines are not seen in the spectra of NGC 40.

The work of Storey (1981) shows that the effective recombination coefficient of Pengelly (1963, see Seaton 1978) should be reliable for λ 4267 and we have seen in Section 3.1 that the (λ 4267)/(λ 1908) ratio gives an electron temperature consistent with temperatures deduced by other methods. We therefore consider the number of quanta in other C II lines relative to the number in λ 4267:

$$q(\lambda) = (\lambda/4267)\,F(\lambda)/F(4267). \qquad (5.1)$$

Table 6 gives values of $q(\lambda)$ for IC 418 and NGC 40 and results of calculations for Case A (optically thin in resonance lines) and Case B (optically thick, resonance lines in radiative detailed balance).

In the calculations of Pengelly, dielectronic recombination was not allowed for and the 'two-electron' transitions $2s^2 3p \rightarrow 2s\,2p^2$ were not considered. We use the results of Pengelly for λ 4267 and λλ 7231, 7236 and for the total rate of population of $2s^2 3p$, and we calculate branching ratios for transitions from $2s^2 3p$ using the transition probabilities of Nussbaumer & Storey (1981a). For λ 1335 we use the effective recombination coefficient of Storey (1981), calculated allowing for dielectronic recombination. Our results for some of the other transitions may be in error due to neglect of dielectronic recombination.

For $2s^2 3d\ ^2D \rightarrow 2s^2 3p\ ^2P^0$ λλ 7231, 7236 there is a large difference between the calculated results for Cases A and B; this is because, for Case A, the $2s^2 3d$ state is depopulated mainly by the resonance transition $2s^2 3d \rightarrow 2s^2 2p$ λ 687. The observed value of $q$(7231, 7236) for NGC 40 is somewhat less than the value for Case B, indicating that λ 687 is not

**Table 6.** Values of $q(\lambda)$, defined by (5.1), for lines of C II.

| λ | Observed | | Calculated | |
|---|---|---|---|---|
| | IC 418 | NGC 40 | Case A | Case B |
| 1335 | 11 | <1.5 | 21 | 21 |
| 1761 | 2 ± 1 | 6 ± 3 | 0.3 | 1.8 |
| 2836 | 2 ± 1 | 4 ± 2 | 0.3 | 1.9 |
| 4267 | 1.0 | 1.0 | 1.0 | 1.0 |
| 7231, 7236 | – | 1.7 ± 0.4 | 0.06 | 3.2 |

fully in detailed balance. The values of $q(1761)$ and $q(2836)$ for IC 418 are close to the calculated values for Case B, whereas those for NGC 40 are somewhat larger. The calculated values may be underestimated due to neglect of the contribution of dielectronic recombination to the rate of population of $2s^2 3p$. The relative strengths of λ 1761 and λ 2836 are consistent with those expected from the calculated branching ratios. Other possible transitions from $2s^2 3p$ are $2s^2 3p\ ^2P^0 \rightarrow 2s^2 3s\ ^2S$ λλ 6578, 6582 and $2s^2 3p\ ^2P^0 \rightarrow 2s 2p^2\ ^2P$ λλ 4738, 4744, for which the Case B calculations give $q(6578, 6582) = 1.5$ and $q(4738, 4744) = 0.003$. The λλ 6578, 6582 lines are blended with [N II] λ 6583, which is stronger by a factor of about 100, and the λλ 4738, 4744 lines are much too weak to be detected.

The λ 1335 lines in IC 418 are discussed by Clavel *et al.* (1981). These resonance lines have large optical depths for scattering, which increases the probability of absorption by dust in the nebula. The observed value of $q(1335)$ for IC 418 is about one half of the value calculated from recombination theory, and Clavel *et al.* showed that this could be explained with an optical depth for absorption by dust of $\tau_D(\text{abs}) = 0.08$. For NGC 40 the observations give $q(1335)$ to be less than a tenth of the calculated value and it is unlikely that this can be explained purely in terms of absorption by internal dust. It is more likely that the strength of λ 1335 is mainly reduced by absorption in interstellar C II lines. The interstellar C II line absorption is expected to be much larger for NGC 40 than for IC 418, both because NGC 40 has a much larger reddening constant $c$ and because IC 418 has a larger radial velocity which leads to a displacement between the wavelengths of the C II emission from the nebula and the interstellar C II absorption.

## 6 The C IV lines

The nebulosity of NGC 40 is of low excitation as judged, for example, by the weakness of the O III lines; our observations give $F(\lambda\lambda 4959, 5007)/F(\text{H}\beta) = 0.24$ and from Table 5 the ionic abundance ratio

$$N(O^{2+})/N(O^{+}) = 0.006. \tag{6.1}$$

It is therefore surprising that C IV λ 1549 is observed to be quite strong. If we assume collisional excitation of C IV and use $T_e = 10\,500$ K we obtain $N(C^{3+})/N(H^{+}) = 5 \times 10^{-5}$ and hence, from Table 5

$$N(C^{3+})/N(C^{2+}) = 0.12. \tag{6.2}$$

Since the ionization potential of $O^{+}$ is 35.1 eV and that of $C^{2+}$ is 47.9 eV we would expect to have $\{N(C^{3+})/N(C^{2+})\} < \{N(O^{2+})/N(O^{+})\}$. This expectation is in agreement with observations for other objects; thus, for example, IC 418 is of higher excitation than NGC 40, with $N(O^{2+})/N(O^{+}) = 0.10$, but C IV λ 1549 is not observed in the offset spectra of Adams & Seaton.

The C IV lines are strong in the spectrum of the central star of NGC 40 and we therefore consider the possibility that the C IV lines in the nebular spectrum are produced by scattering. We can rule out the possibility of scattering by dust, or instrumental scattering, since other strong stellar lines, such as C III λ 2297, are not seen in the nebular spectra. This leaves the possibility of resonance scattering in the C IV lines. If we assume that $N(C^{3+})/N(C^{2+}) = N(O^{2+})/N(O^{+})$ we find that the optical depth at the centre of the λ 1548 line is $\tau_0 \sim 10$ for the bright patch observed with *IUE*; it follows that the patch may be optically thick for scattering in the resonance lines. Let $L_\lambda$ be the luminosity of the central star per unit wavelength at wavelength λ and let the patch of nebulosity subtend a solid angle Ω at the star.

The luminosity of scattered radiation is

$$L(\text{scatt}) = \frac{\Omega}{4\pi} L_\lambda \Delta\lambda \tag{6.3}$$

where $\Delta\lambda$ is the width of the scattered line and $L_\lambda$ the luminosity of the star. If the scattering is isotropic we have

$$F(\text{scatt}) = \frac{\Omega}{4\pi} F_\lambda \Delta\lambda \tag{6.4}$$

where $F(\text{scatt})$ is the observed scattered flux and $F_\lambda$ the observed stellar flux. We obtain an approximate upper limit for $F(\text{scatt})$.

Fig. 10 shows the C IV P-Cygni feature from the spectra of the central star obtained by Benvenuti *et al.* (1981). Allowing for the fact that this profile is not completely resolved, we estimate that at the maximum of the emission feature $F_\lambda = 3 \times 10^{-12}\,\text{erg cm}^{-2}\,\text{s}^{-1}\,\text{Å}^{-1}$. We obtained an upper limit to $F(\text{scatt})$ using the maximum value of $F_\lambda$.

From inspection of Fig. 1 we estimate that, in (6.4), $(\Omega/4\pi) \simeq 0.10$. The width $\Delta\lambda$ in (6.4) is given by $(\Delta\lambda/\lambda) = \Delta v/c$, where $\Delta v$ is the spread in velocity for the region in which scattering occurs. The maximum expansion velocity for NGC 40 is $v = 29\,\text{km s}^{-1}$. We take $\Delta v \simeq 20\,\text{km s}^{-1}$, so $\Delta\lambda \simeq 0.10$ Å. Allowing for the two C IV line components, $\lambda$ 1548.2 and $\lambda$ 1550.8, we obtain from (6.4) $F(\text{scatt}) = 6 \times 10^{-14}\,\text{erg cm}^{-2}\,\text{s}^{-1}$. The observed flux is, from Table 2, $F(\lambda 1549) = 5.3 \times 10^{-13}\,\text{erg cm}^{-2}\,\text{s}^{-1}$, and hence too large to be explained by the scattering mechanism.

We have looked for other features which might provide checks on the $C^{3+}$ abundance. The C III $\lambda$ 2297 dielectronic recombination line could give the $C^{3+}$ abundance directly and the ratio $F$(N IV] $\lambda$ 1486)/$F$(N III] 1749) could provide information on the $C^{3+}/C^{2+}$ ionization equilibrium. Unfortunately the lines concerned, $\lambda\lambda$ 2297, 1486 and 1749, are too weak for useful results to be obtained.

A clue to the origin of the C IV radiation may be provided by the off-set spectrum obtained by Benvenuti *et al.* (1981) at a position 7.5 arcsec north of the star, and a position

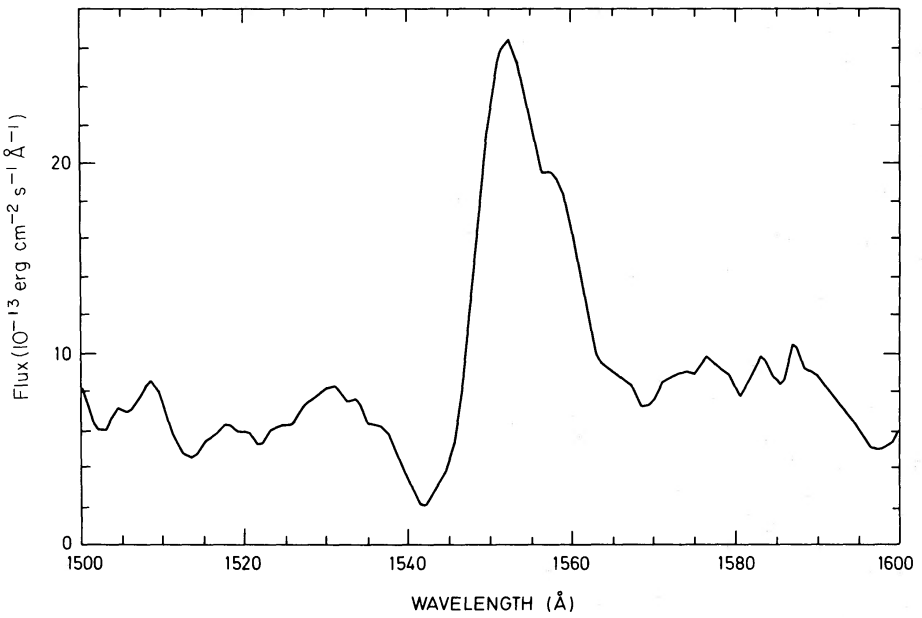


**Figure 10.** The C IV P-Cygni profile in the central star of NGC 40, from the spectrum obtained by Benvenuti *et al.* (1981).

angle similar to that used in our work. Their offset spectrum, compared with ours, contains more radiation from the central region of the nebula. Their spectrum gives $F(\lambda 1549) = 1.0 \times 10^{-12}$ erg cm$^{-2}$ s$^{-1}$ compared with $5.3 \times 10^{-13}$ erg cm$^{-2}$ s$^{-1}$ for ours. We estimate, from Fig. 1, that the H$\beta$ flux for their position is about one half of that for ours. Our value of $F(\lambda 1549)/F(\mathrm{H}\beta)$ is 0.26 and we estimate the ratio for their position is 1.0. It is seen that C IV is stronger, both absolutely and relative to H$\beta$, in the inner regions of the nebula. It would be of interest to have optical observations for these regions in order to establish whether one obtains consistent values of $O^{2+}/O^{+}$ and $C^{3+}/C^{2+}$ ratios, assuming C IV $\lambda$ 1549 to be collisionally excited. A possible explanation for the strength of C IV $\lambda$ 1549 from the bright patch which we have observed is that radiation produced in the inner region is scattered by the patch. This mechanism will be most effective if velocity gradients are small.

Problems concerning the C IV $\lambda$ 1549 emission from the nebulosity of NGC 40 may be summarized as follows. (i) Assuming the C IV emission from the bright patch to be produced by collisional excitation, one obtains a $C^{3+}/C^{2+}$ ratio which is difficult to reconcile with the $O^{2+}/O^{+}$ ratio, but which is still sufficiently small as not to affect significantly our deduced C abundance. (ii) Scattering of radiation from the central star cannot explain all of the C IV radiation from the patch. There may be a contribution from scattering of radiation produced in the inner part of the nebula. (iii) The total C IV emission from the nebulosity of NGC 40 is much larger than that from other low-excitation nebulae such as, for example, IC 418. This suggests that the emission from NGC 40 is due to its having a carbon-rich central star with a strong stellar wind.

A clue to the existence of unusual dynamics in NGC 40 may be provided by the expansion velocity measurements of Sabbadin & Hamzaoglu (1982). They derived velocities of 23, 27 and 29 km s$^{-1}$ for H$\alpha$, [N II] and [O III] respectively. Such a trend is unusual, because for most nebulae the measured expansion velocity for high-ionization species is less than that for low-ionization species. It would be of interest to make a study of the interaction of the wind with the nebulosity.

## 7 Conclusions

(i) The WC8 central star of NGC 40 has the remarkable abundance ratio C/He ~ 0.2 and probably no hydrogen. The envelope of NGC 40 has abundances which are not abnormal for a planetary nebula. The composition of the stellar atmosphere has presumably changed subsequent to the ejection of the nebular shell.

(ii) Interpretation of the ratio (C III] $\lambda$ 1908)/C II $\lambda$ 4267), assuming $\lambda$ 1908 to be excited by collisions and $\lambda$ 4267 by recombination, gives an electron temperature $T_e$ (C III) which is satisfactory in that it is intermediate between $T_e$ (N II) and $T_e$ (O III). A number of other C II recombination lines are identified and discussed.

(iii) The flux in C IV $\lambda$ 1549 from the nebular envelope is too large for production by normal processes of thermal excitation. Processes of scattering of $\lambda$ 1549 are discussed. It is probable that production of $\lambda$ 1549 in the envelope is due to processes involving the wind from the central star.

## Acknowledgments

We are grateful to Dr N. K. Reay for providing the H$\beta$ map of NGC 40 and to Dr J. P. Harrington for providing a computer program used to calculate the nebular continuum. Our *IUE* observations were obtained at the VILSPA tracking station of the European Space Agency. RESC was supported by the UK Science and Engineering Research Council.

## References


Adams, S. & Seaton, M. J., 1983. *Mon. Not. R. astr. Soc.,* to be submitted.
Aller, L. H. & Czyzak, S. J., 1979. *Astrophys. Space Sci.,* **62,** 397.
Aller, L. H., Czyzak, S. J., Buerger, E. G. & Lee, P., 1972. *Astrophys. J.,* **172,** 361.
Baluja, K. L., Burke, P. G. & Kingston, A. E., 1981. *J. Phys. B.,* **14,** 119.
Barker, T., 1979. *Astrophys. J.,* **227,** 863.
Benvenuti, P., Perinotto, M. & Willis, A. J., 1981. *Proc. IAU Sym. 99,* Cozumel, Mexico.
Berrington, K. A. & Burke, P. G., 1981. *Planet. Space Sci.,* **29,** 377.
Brocklehurst, M., 1971. *Mon. Not. R. astr. Soc.,* **153,** 471.
Brocklehurst, M., 1972. *Mon. Not. R. astr. Soc.,* **157,** 211.
Clavel, J., Flower, D. R. & Seaton, M. J., 1981. *Mon. Not. R. astr. Soc.,* **197,** 301.
Harrington, J. P., Lutz, J. H., Seaton, M. J. & Stickland, D. J., 1980. *Mon. Not. R. astr. Soc.,* **191,** 13.
Harrington, J. P., Seaton, M. J., Adams, S. & Lutz, J. H., 1982. *Mon. Not. R. astr. Soc.,* **199,** 517.
Higgs, L. A., 1971. *Catalog of Radio Observations of Planetary Nebulae and Related Optical Data,* National Research Council Canada, NRC-12129.
Jackson, A. R. G., 1973. *Mon. Not. R. astr. Soc.,* **165,** 53.
Kaler, J. B., 1978. *Astrophys. J.,* **226,** 947.
Lambert, D. L. & Luck, R. E., 1978. *Mon. Not. R. astr. Soc.,* **183,** 79.
Liller, W., 1955. *Astrophys. J.,* **122,** 240.
Louise, R., 1981. *Astr. Astrophys.,* **102,** 303.
Mendoza, C. & Zeippen, C., 1982. *Mon. Not. R. astr. Soc.,* **198,** 127.
Natta, A., Panagia, N & Preite-Martinez, A., 1980. *Astr. Astrophys.,* **242,** 596.
Nussbaumer, H. & Rusca, C., 1979. *Astr. Astrophys.,* **72,** 129.
Nussbaumer, H. & Storey, P. J., 1981a. *Astr. Astrophys.,* **96,** 91.
Nussbaumer, H. & Storey, P. J., 1981b. *Astr. Astrophys.,* **99,** 177.
Oke, J. B., 1974. *Astrophys. J. Suppl.,* **27,** 21.
Osterbrock, D. E., 1960. *Astrophys. J.,* **131,** 541.
Osterbrock, D. E., 1974. *Astrophysics of Gaseous Nebulae,* Freeman, San Francisco.
Pengelly, M., 1963. *PhD thesis,* University of London.
Pottasch, S. R., Wesselius, P. R., Wu, C.-C. & van Duinen, R. J., 1977. *Astr. Astrophys.,* **54,** 435.
Pottasch, S. R., Wesselius, P. R., Wu, C.-C., Fieten, H. & van Duinen, R. J., 1978. *Astr. Astrophys.,* **62,** 95.
Sabbadin, F. & Hamzaoglu, E., 1982. *Astr. Astrophys.,* **109,** 131.
Saraph, H. E. & Seaton, M. J., 1970. *Mon. Not. R. astr. Soc.,* **148,** 367.
Savage, B. D. & Mathis, J. S., 1979. *A. Rev. astro. Astrophys.,* **17,** 73.
Seaton, M. J., 1975. *Mon. Not. R. astr. Soc.,* **170,** 475.
Seaton, M. J., 1978. *Planetary Nebulae,* p. 131, ed. Terzian, Y., Reidel, Dordrecht, Holland.
Seaton, M. J., 1979. *Mon. Not. R. astr. Soc.,* **185,** 57P.
Stone, R. P. S., 1977. *Astrophys. J.,* **218,** 267.
Storey, P. J., 1981. *Mon. Not. R. astr. Soc.,* **195,** 27P.
Torres-Peimbert, S. & Peimbert, M., 1977. *Rev. Mexicana astr. Astrofiz,* **2,** 181.
Zeippen, C., 1982. *Mon. Not. R. astr. Soc.,* **198,** 111.